Asociación Argentina
de Mecánica Computacional

Mecánica Computacional Vol XXVI, pp.2820-2831
Sergio A. Elaskar, Elvio A. Pilotta, Germán A. Torres (Eds.)
Córdoba, Argentina, Octubre 2007

DYNAMIC STABILITY ANALYSIS OF ISOLATED INTEGRATED MOTOR PROPULSOR

Sergio Preidikman[a], Patricio Ravetta[b], and Ricardo Burdisso[c]

[a] *Departamento de Estructuras, F. C. E. F. y N, Universidad Nacional de Córdoba, Casilla de Correo 916, 5000 Córdoba, Argentina, spreidik@vt.edu, www.efn.uncor.edu*
[b] *AVEC, Inc., 2000 Kraft Drive, Suite 1109, Virginia Tech Corporate Research Center, Blacksburg, VA, 24060, USA, pravetta@avec-engineering.com, www.avec-engineering.com*
[b] *Department of Mechanical Engineering, Virginia Polytechnic Institute and State University, Blacksburg, VA, 24061-0238, USA, rburdiss@vt.edu, www.me.vt.edu*

Keywords: Integrated Motor Propulsors, Dynamic Stability, Fluid-Structure interaction.

Abstract. Integrated Motor Propulsors (IMP) are being considered for the propulsion system of future underwater vehicles. A key issue is the reduction of IMP mechanical vibration transmitted to the vehicle. To this end, vibration isolation of the IMP is a potential approach to reduce these vibrations. However, the isolation of the IMP from the vehicle body can potentially lead to a dynamic instability problem of the system. Coupled-mode flutter of aircraft wings is an example of such dynamic instability caused by the interaction of a flow with a flexible structure. For the particular case of the IMP, the instability occurs because the thrust generated by the IMP creates a static load that is always aligned with one of the IMP axes which is connected to the vehicle's body through a compliant mount. This results in a following force acting on a flexible system much like a loose garden hose. The objective of this work is to develop the theoretical formulation to analyze the dynamic stability of soft mounted IMP systems, and to develop numerical tools and software to perform numerical simulations of the dynamic stability of soft mounted IMP systems taking into account the external fluid-loading effects. The approach here was to develop a generic, closed form modeling tool of the isolated IMP system to determine the dynamic stability of the system. The model includes the most important system parameters, e.g. IMP dynamic properties, isolation properties, fluid loading, and so forth. The formulation was numerically implemented in a computer code and examples will be presented. The stability of the system can be determined by inspection of the time history responses and/or an eigenvalue analysis, e.g. coalescence of natural frequencies. The data for these examples do not correspond to any particular IMP. However, the tool developed here can be used to analyze practical cases.

Copyright @ 2007 Asociación Argentina de Mecánica Computacional
http://www.amcaonline.org.ar

1 INTRODUCTION

Integrated Motor Propulsors (IMP) are electric integrated thruster devices being considered for the propulsion system of underwater vehicles for military, industrial, and scientific applications (Brown et.al., 1989; Abu Sharkh et.al., 2004). A key issue is the reduction of IMP mechanical vibration transmitted to the vehicle. To this end, vibration isolation of the IMP is a potential approach to reduce these vibrations. However, the isolation of the IMP from the vehicle body can potentially lead to a dynamic instability problem of the system (Rocard and Meyer, 1958; Xie, 2006). Flutter of aircraft wings is an example of instability caused by the interaction of a flow with a flexible structure (Milne-Thomson, 1958).

In the present situation, the instability occurs because the thrust generated by the IMP creates a static load that is always aligned with the IMP axis which is connected to the vehicle's body through a compliant mount. This results in a following force acting on a flexible system much like a loose garden hose. It is interesting to note that this instability was observed in preliminary experiments.

The objective of this work is to develop the theoretical formulation for the dynamic stability analysis of soft mounted IMP systems. The approach is to develop a simple but effective closed form solution to the problem, e.g. rather than using time consuming numerical methods. The formulation was programmed and numerical examples are presented to illustrate the approach. The data for these examples do not correspond to any particular IMP. However, the tool developed here can be used to analyze practical cases.

2 MODELING APPROACH

The approach here is to develop a "generic" model of an isolated IMP system including its key parameters. Figure 1 illustrates an IMP isolated from a vehicle's body, e.g. torpedo.

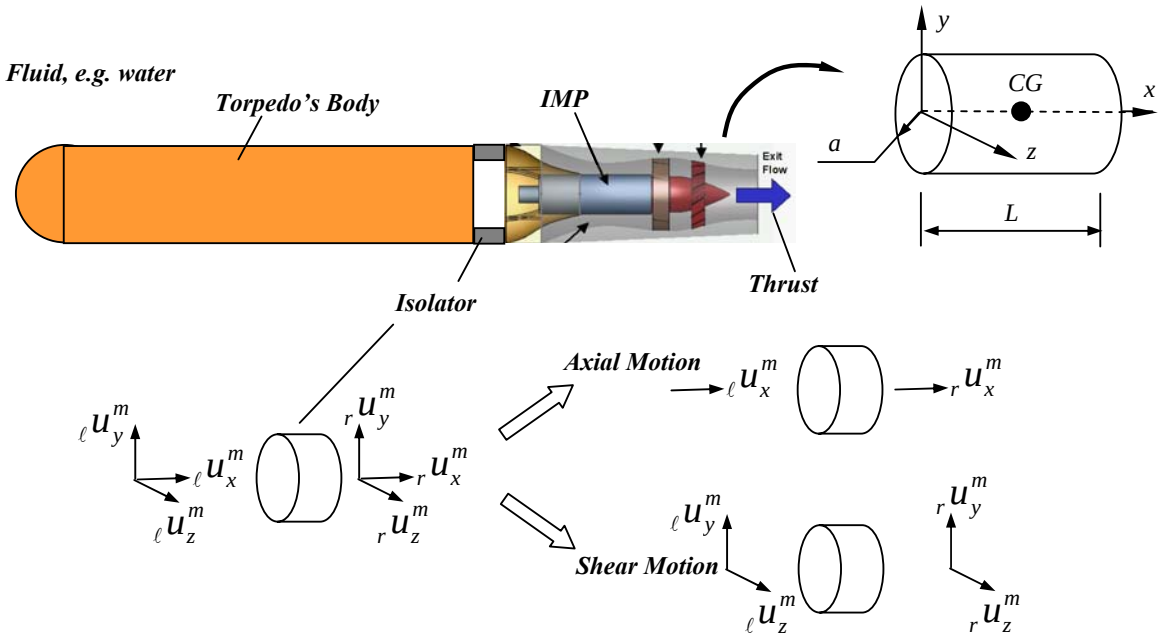

Figure 1: Example of an isolated IMP.

The model consists of basic components such as the IMP, the isolation, the vehicle body

the IMP is attached to, and the surrounding fluid. The IMP is modeled as a rigid cylindrical body of length *L* and radius *a* as shown in Figure 1. The motion of the IMP will be defined in terms of the translation and rotation vectors, $\left(u_x, u_y, u_z\right)$ and $\left(\phi_x, \phi_y, \phi_z\right)$, respectively. The dynamics of the IMP are then defined simply in terms of its mass and the polar moments of inertia , e.g. M_{IMP} = mass, J^x_{IMP}, I^y_{IMP}, and I^z_{IMP} = polar moment of inertia about the *x, y,* and *z*-axis through the center of gravity (***cg***), respectively. The fluid inside the IMP is assumed to be at rest and accounted for in the mass properties.

The effect of the external fluid on the dynamics of the IMP (e.g. fluid loading effects) will be incorporated through equivalent mass and moment of inertias, e.g. $M_{Fluid-IMP}$ = added fluid-IMP mass, $I^y_{Fluid-IMP}$ and $I^z_{Fluid-IMP}$ = added fluid second moment of inertia about the *y* and *z*-axis through the ***cg.*** Note that since the fluid is assumed inviscid, it does not contribute to the mass in the *x*-direction and polar moment of inertia about the *x*-axis. Once again the fluid will be assumed to be at rest. To find the fluid inertial terms, the equivalent fluid mechanical-impedance terms are determined from the closed form solution of a cylinder embedded in a baffle as shown in Figure 2. The IMP will then be allowed to independently move in the u_y and ϕ_y directions and the equivalent mechanical impedance terms computed.

Finally, it is important to remark that the dynamics of the spinning propeller is not taken into account in this model (sometimes referred as Coriolis effect).

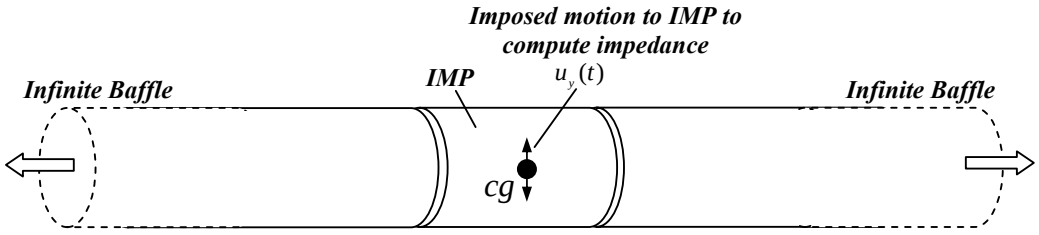

Figure 2: Illustration of the approach to account for the effect of the fluid on the IMP dynamics.

The isolation mounts are modeled as simple homogenous, isotropic, cylindrical-shaped, viscous mounts as shown in Figure 1. The motion of the mounts will be defined in terms of the translation and rotation of the two ends of the mount (referred as left and right ends) defined by $\left({}_\ell u^m_x, {}_\ell u^m_y, {}_\ell u^m_z, {}_\ell \phi^m_x, {}_\ell \phi^m_y, {}_\ell \phi^m_z\right)$ and $\left({}_r u^m_x, {}_r u^m_y, {}_r u^m_z, {}_r \phi^m_x, {}_r \phi^m_y, {}_r \phi^m_z\right)$, respectively. The dynamics of the mounts is then defined by a 12x12 fully coupled dynamic stiffness matrix. This matrix can be computed using numerical methods such as finite elements. However, this approach is beyond the scope of this work and a simplified model is used here. To this end, the mounts are assumed massless and to have uncoupled axial and shear motions. The dynamics of the isolator are defined by the axial and shear stiffness and equivalent viscous damping coefficients, e.g. k^m_x, k^m_s, c^m_s and c^m_x. Note that the system of three vibration isolators has 18 degrees of freedom (dof), i.e. 6 dof per isolator. However, since the vibration absorbers are linked to a rigid body, the actual number of degrees of freedom is reduced to only 6. This fact was accounted for using static condensation (Guyan condensation) as will be explained in following sections (Meirovitch, 1970; Baruh, 1999, and 1980).

The vehicle's body is assumed rigid as well as to have a mass much larger than the IMP.

This assumption allows the modeling of the vehicle's body as a fixed boundary condition at the end of the isolators, e.g. the motion at the left mount boundary vanishes.

The main components of the analytical model are described in the following subsections.

2.1 Kinematics of Model

The kinematics of the IMP is described using two reference systems: one is fixed to the vehicle's body (*N*) and considered to be an inertial reference frame, and the other is fixed to and moves with the IMP's body (*A*) in such a way that the coordinates of points in the body do not change with time. These two reference systems and a generic IMP are represented in Figure 3a.

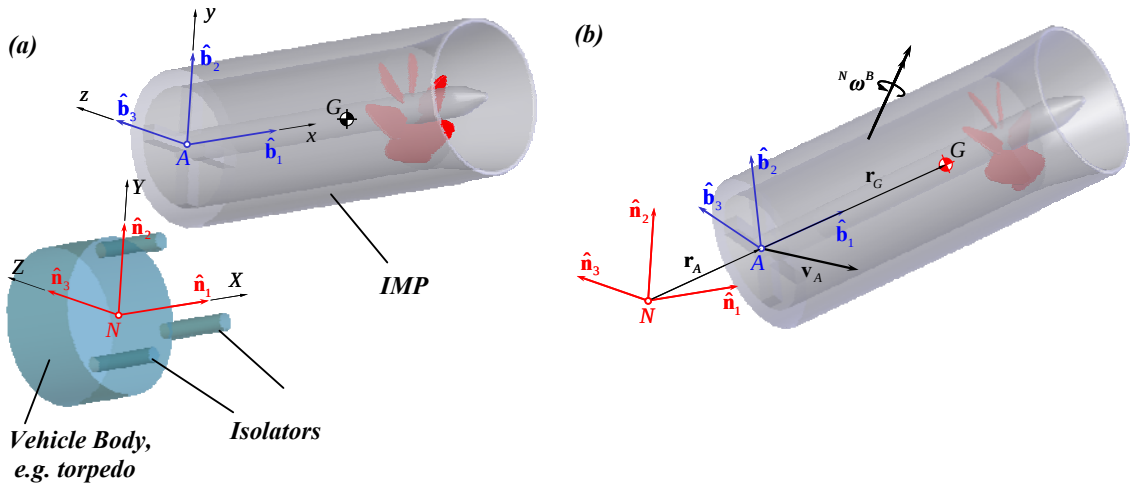

Figure 3: (a) Coordinate systems and (b) IMP motion.

Point *N* is the origin of the torpedo-fixed (Newtonian) coordinate system, point *A* is the origin of the moving coordinate system, and point *G* is at the center of mass of the IMP. From Figure 3b, the position vector of point *A* is expressed as $\mathbf{r}_A = \{X_A, Y_A, Z_A\}^T$. The velocity of point *A* with respect to the Newtonian system is given as

$$ {}^N\mathbf{v}_A = \frac{{}^N d}{dt}\mathbf{r}_A = \{\dot{X}_A, \dot{Y}_A, \dot{Z}_A\}^T \tag{1} $$

where the superscript *N* indicates that these are the components in the Newtonian system. It is also convenient to express the same velocity in terms of its components in the body-fixed system as

$$ {}^B\mathbf{v}_A = \{u, v, w\}^T \tag{2} $$

where the superscript *B* indicates that these are the components in the body-fixed system. Because *u*, *v*, and *w* are not the derivatives of coordinates, the two sets of components need to be related. The orientation of the body with respect to the vehicle's body is described by means of three Euler angles. Beginning with the two coordinate systems aligned, the IMP is rotated about the *z*-axis ($\hat{\mathbf{b}}_3$-axis) through the angle ψ, next the IMP is rotated about the new position of the *y*-axis ($\hat{\mathbf{b}}_2$-axis) through the angle θ, and finally the IMP is rotated about the

latest position of the *x*-axis ($\hat{\mathbf{b}}_1$-axis) through the angle ϕ. Then, the two sets of velocity components for ${}^{N}\mathbf{v}_A$ are related as

$$ {}^{N}\mathbf{v}_A = \mathbf{J}_1\left(\boldsymbol{\Xi}\right) {}^{B}\mathbf{v}_A \tag{3} $$

where $\boldsymbol{\Xi} = \{\phi, \theta, \psi\}^T$ and

$$ \mathbf{J}_1\left(\boldsymbol{\Xi}\right) = \begin{bmatrix} \cos\psi\cos\theta & -\sin\psi\cos\phi + \cos\psi\sin\theta\sin\phi & \sin\psi\sin\phi + \cos\psi\cos\phi\sin\theta \\ \sin\psi\cos\theta & \cos\psi\cos\phi + \sin\psi\sin\theta\sin\phi & -\cos\psi\sin\phi + \sin\psi\sin\theta\cos\phi \\ -\sin\theta & \cos\theta\sin\phi & \cos\theta\cos\phi \end{bmatrix} \tag{4} $$

The acceleration of point *A* with respect to the fixed coordinate system expressed in terms of its components in the body-fixed coordinate system is given by

$$ {}^{N}\mathbf{a}_A = \frac{{}^{N}d^2}{dt^2}\mathbf{r}_A = \begin{Bmatrix} \dot{u} \\ \dot{v} \\ \dot{w} \end{Bmatrix} + {}^{N}\boldsymbol{\omega}^{B} \times {}^{B}\mathbf{v}_A = \begin{Bmatrix} \dot{u} + q\,w - r\,v \\ \dot{v} + r\,u - p\,w \\ \dot{w} + p\,v - q\,u \end{Bmatrix} \tag{5} $$

where ${}^{N}\boldsymbol{\omega}^{B} = \{p, q, r\}^T$ is the angular velocity of the IMP expressed in terms of its components in the body-fixed system. The components of ${}^{N}\boldsymbol{\omega}^{B}$ are related to the derivatives of the Euler angles as follows

$$ \dot{\boldsymbol{\Xi}} = \mathbf{J}_2\left(\boldsymbol{\Xi}\right) {}^{N}\boldsymbol{\omega}^{B} \tag{6} $$

where

$$ \mathbf{J}_2\left(\boldsymbol{\Xi}\right) = \begin{bmatrix} 1 & \sin\phi\tan\theta & \cos\phi\tan\theta \\ 0 & \cos\phi & -\sin\phi \\ 0 & \dfrac{\sin\phi}{\cos\theta} & \dfrac{\cos\phi}{\cos\theta} \end{bmatrix} \tag{7} $$

The velocity of the center of mass, *G*, with respect to the ground expressed in terms of its components in the body-fixed system, is given by

$$ {}^{B}v_G = {}^{B}\mathbf{v}_A + {}^{N}\boldsymbol{\omega}^{B} \times \mathbf{r}_G = \begin{Bmatrix} u + q\,z_G - r\,y_G \\ v + r\,x_G - p\,z_G \\ w + p\,y_G - q\,x_G \end{Bmatrix} \tag{8} $$

where $\mathbf{r}_G = \{x_G, y_G, z_G\}^T$ is the position of the center of mass with respect to point *A*, expressed in terms of its components in the body-fixed system.

Finally, the acceleration of the center of mass with respect to the ground expressed in terms of its components in the body-fixed system is given by

$$
\begin{aligned}
{}^{B}\mathbf{a}_{G} &= \begin{Bmatrix} \dot{u} + \dot{q}\, z_G - \dot{r}\, y_G \\ \dot{v} + \dot{r}\, x_G - \dot{p}\, z_G \\ \dot{w} + \dot{p}\, y_G - \dot{q}\, x_G \end{Bmatrix} + {}^{N}\boldsymbol{\omega}^{B} \times {}^{B}\mathbf{v}_{G} \\
&= \begin{Bmatrix} u - v\, r + w\, q - x_G\left(q^2 + r^2\right) + y_G\left(p\, q - r\right) + z_G\left(p\, r - q\right) \\ v - w\, p + u\, r - y_G\left(r^2 + p^2\right) + z_G\left(q\, r - p\right) + x_G\left(q\, p + r\right) \\ w - u\, q + v\, p - z_G\left(p^2 + q^2\right) + x_G\left(r\, p - q\right) + y_G\left(r\, q + p\right) \end{Bmatrix}
\end{aligned} \tag{9}
$$

where $\left\{\dot{p}, \dot{q}, \dot{r}\right\}^{T} = {}^{N}\boldsymbol{\alpha}^{B}$ is the angular acceleration of the IMP.

The transformations can be placed in a single expression as follows

$$
\dot{\boldsymbol{\eta}} = \begin{Bmatrix} \dot{\mathbf{r}}_A \\ \dot{\boldsymbol{\Xi}} \end{Bmatrix} = \begin{Bmatrix} \dot{X}_A \\ \dot{Y}_A \\ \dot{Z}_A \\ \dot{\phi} \\ \dot{\theta} \\ \dot{\psi} \end{Bmatrix} = \left[\begin{array}{c|c} \mathbf{J}_1\left(\boldsymbol{\Xi}\right) & \mathbf{0}_{3\times 3} \\ \hline \mathbf{0}_{3\times 3} & \mathbf{J}_2\left(\boldsymbol{\Xi}\right) \end{array}\right] \begin{Bmatrix} u \\ v \\ w \\ p \\ q \\ r \end{Bmatrix} = \mathbf{J} \begin{Bmatrix} {}^{B}\mathbf{v}_A \\ \boldsymbol{\omega} \end{Bmatrix} = \mathbf{J}\ \boldsymbol{\nu} \tag{10}
$$

where $\mathbf{0}_{3\times 3}$ is the 3×3 null matrix.

2.2 Dynamics of Model

The equations used to determine the motion of the body are now described. The equations of motion are written in the following form

$$
m\ \mathbf{a}_G = \mathbf{F} \tag{11}
$$

where m is the mass of the body, $\mathbf{a}_G$ is the acceleration of its center of mass (as obtained in the previous section), and $\mathbf{F} = \left\{F_x, F_y, F_z\right\}^{T}$ is the resultant force acting on the body expressed in terms of its components in the body-fixed system. The remaining equations of motion are given by

$$
\bar{\mathbf{I}}_A\ {}^{N}\boldsymbol{\alpha}^{B} + {}^{N}\boldsymbol{\omega}^{B} \times \left(\bar{\mathbf{I}}_A\ {}^{N}\boldsymbol{\omega}^{B}\right) + m\, \mathbf{r}_G \times \mathbf{a}_A = \mathbf{M}_A \tag{12}
$$

where ${}^{N}\boldsymbol{\alpha}^{B}$ is the angular acceleration of the IMP, ${}^{N}\boldsymbol{\omega}^{B}$ is the angular velocity (as obtained in the previous section), $\mathbf{a}_A$ is the acceleration of point A (as obtained in the previous section), $\mathbf{M}_A = \left\{M_x, M_y, M_z\right\}^{T}$ is the resultant moment about point A, expressed in terms of its components in the body-fixed system, and $\bar{\mathbf{I}}_A$ is the inertia tensor for point A in the body-fixed coordinate system given by

$$
\bar{\mathbf{I}}_A = \begin{bmatrix} I_{xx}^{A} & -I_{xy}^{A} & -I_{xz}^{A} \\ -I_{xy}^{A} & I_{yy}^{A} & -I_{yz}^{A} \\ -I_{xz}^{A} & -I_{yz}^{A} & I_{zz}^{A} \end{bmatrix} = \bar{\mathbf{I}}_G + m\left[\left(\boldsymbol{\pi}\cdot\boldsymbol{\pi}\right)\bar{\mathbf{U}} - \left(\boldsymbol{\pi}\otimes\boldsymbol{\pi}\right)\right] \tag{13}
$$

where $\bar{\mathbf{I}}_G$ is the inertia tensor for point G in the body-fixed coordinate system, $\bar{\mathbf{U}}$ is the

second-order unit (or identity) tensor, $\boldsymbol{\pi} = -\mathbf{r}_G$ (see Figure 3), and $\boldsymbol{\pi} \otimes \boldsymbol{\pi}$ is the tensor product of vector $\boldsymbol{\pi}$. Writing equations (11) and (12) in terms of their components yields

$$\begin{aligned} m\left[\dot{u} - v\,r + w\,q - x_G\left(q^2 + r^2\right) + y_G\left(p\,q - \dot{r}\right) + z_G\left(p\,r - \dot{q}\right)\right] &= F_x \\ m\left[\dot{v} - w\,p + u\,r - y_G\left(r^2 + p^2\right) + z_G\left(q\,r - \dot{p}\right) + x_G\left(q\,p + \dot{r}\right)\right] &= F_y \\ m\left[\dot{w} - u\,q + v\,p - z_G\left(p^2 + q^2\right) + x_G\left(r\,p - \dot{q}\right) + y_G\left(r\,q + \dot{p}\right)\right] &= F_z \end{aligned} \tag{14}$$

and

$$\begin{aligned} I_{xx}^A\,\dot{p} + \left(I_{zz}^A - I_{yy}^A\right)q\,r - \left(\dot{r} + p\,q\right)I_{xz}^A + \left(r^2 - q^2\right)I_{yz}^A + \left(p\,r - \dot{q}\right)I_{xy}^A + \\ + m\left[y_G\left(\dot{w} - u\,q + v\,p\right) - z_G\left(\dot{v} - w\,p + u\,r\right)\right] = M_x \\ I_{yy}^A\,\dot{q} + \left(I_{xx}^A - I_{zz}^A\right)r\,p - \left(\dot{p} + q\,r\right)I_{xy}^A + \left(p^2 - r^2\right)I_{xz}^A + \left(q\,p - \dot{r}\right)I_{yz}^A + \\ + m\left[z_G\left(\dot{u} - v\,r + w\,q\right) - x_G\left(\dot{w} - u\,q + v\,p\right)\right] = M_y \\ I_{zz}^A\,\dot{r} + \left(I_{yy}^A - I_{xx}^A\right)p\,q - \left(\dot{q} + r\,p\right)I_{yz}^A + \left(q^2 - p^2\right)I_{xy}^A + \left(r\,q - \dot{p}\right)I_{xz}^A + \\ + m\left[x_G\left(\dot{v} - w\,p + u\,r\right) - y_G\left(\dot{u} - v\,r + w\,q\right)\right] = M_z \end{aligned} \tag{15}$$

These equations of motion can be rewritten in the following convenient form

$$\mathbf{M}_{RB}\,\dot{\mathbf{v}} = \mathbf{L} - \mathbf{C}_{RB}\left(\mathbf{v}\right)\mathbf{v} \tag{16}$$

where $\mathbf{M}_{RB}$ is the unique, constant, inertia matrix given by

$$\mathbf{M}_{RB} = \left[\begin{array}{ccc|ccc} m & 0 & 0 & 0 & m\,z_G & -m\,y_G \\ 0 & m & 0 & -m\,z_G & 0 & m\,x_G \\ 0 & 0 & m & m\,y_G & -m\,x_G & 0 \\ \hline 0 & -m\,z_G & m\,y_G & I_{xx}^A & -I_{xy}^A & -I_{xz}^A \\ m\,z_G & 0 & -m\,x_G & -I_{xy}^A & I_{yy}^A & -I_{yz}^A \\ -m\,y_G & m\,x_G & 0 & -I_{xz}^A & -I_{yz}^A & I_{zz}^A \end{array}\right] \tag{17}$$

$\mathbf{C}_{RB}$ is a nonunique, time-varying matrix given by

$$\mathbf{C}_{RB} = \left[\begin{array}{c|c} \mathbf{0}_{3\times 3} & \mathbf{C}_{12} \\ \hline \mathbf{C}_{21} & \mathbf{C}_{22} \end{array}\right] \tag{18}$$

where

$$\mathbf{C}_{12} = m\begin{bmatrix} y_G\, q + z_G\, r & -x_G\, q + w & -x_G\, r - v \\ -y_G\, p - w & z_G\, r + x_G\, p & -y_G\, r + u \\ -z_G\, p + v & -z_G\, q - u & x_G\, p + y_G\, q \end{bmatrix}$$

$$\mathbf{C}_{21} = m\begin{bmatrix} -y_G\, q - z_G\, r & y_G\, p + w & z_G\, p - v \\ x_G\, q - w & -z_G\, r - x_G\, p & z_G\, q + u \\ x_G\, r + v & y_G\, r - u & -x_G\, p - y_G\, q \end{bmatrix} = -\mathbf{C}_{12}^T \tag{19}$$

$$\mathbf{C}_{22} = \begin{bmatrix} 0 & -I_{yz}^A\, q - I_{xz}^A\, p - I_{zz}^A\, r & I_{yz}^A\, r + I_{xy}^A\, p - I_{yy}^A\, q \\ -I_{yz}^A\, q + I_{xz}^A\, p - I_{zz}^A\, r & 0 & -I_{xz}^A\, r - I_{xy}^A\, q + I_{xx}^A\, p \\ -I_{yz}^A\, r - I_{xy}^A\, p + I_{yy}^A\, q & I_{xz}^A\, r + I_{xy}^A\, q - I_{xx}^A\, p & 0 \end{bmatrix}$$

and $\mathbf{L}$ is the vector of loads given by

$$\mathbf{L} = \left\{F_x, F_y, F_z, M_x, M_y, M_z\right\}^T \tag{20}$$

Equations (10) and (16) are to be integrated simultaneously. Generally, the procedure is to integrate (16) to find $\boldsymbol{\nu}$ and then to integrate (10) to find $\boldsymbol{\eta}$. The method presented in this work was developed to solve problems for which the components of $\mathbf{L}$ depend on $\boldsymbol{\eta}$, $\boldsymbol{\nu}$, $\dot{\boldsymbol{\nu}}$, and t (time); thus, the acceleration, $\dot{\boldsymbol{\nu}}$, appears on both sides of the governing equations, explicitly on the left-hand side and implicitly in the force terms on the right-hand side. For application to ships and torpedoes, this dependence produces the so-called added-inertia terms, which appear to increase the mass as well as the moments and products of inertia of the body. Of course, the appearance of $\dot{\boldsymbol{\nu}}$ on both sides of the equations creates problems for the traditional numerical schemes, especially when the added mass itself depends on the motion of the body and changes with time, as in the case of ships. The numerical integration scheme to be used is the Hammings-Gill modified-predictor-corrector algorithm that was developed to handle this case.

2.3 Vibration Isolators

As mentioned before, the system of three vibration isolators has 18 degrees of freedom (dof), i.e. 6 dof per isolator. However, since the vibration isolators are linked to a rigid body, the actual number of degrees of freedom is reduced to 6. This fact will be accounted by considering the IMP's center of mass, G, as the "master node" and the three nodes where the isolator connects to the IMP as "slave nodes". This idea allows to connect some dof (so-called "slave" dof) to corresponding dof (according to their physical meaning) of another dof manager (so-called "master" dof). The master-slave principle allows simple modeling of the torpedo-isolators-IMP structure, where multiple elements are connected by introducing multiple nodes sharing displacement/rotations dofs. As a result, the dynamics of the vibration isolators (modeled as beams) is coupled with the dynamics of the IMP. This is accomplished by introducing the effect of the isolators, through a stiffness and damping matrix, as a load term in eq.(20), i.e. forces and moments at point A. In order to relate the master dof (i.e., the dof of the IMP's center of mass) to the slave dof (i.e. the dof of the points where the vibration isolators are attached to the IMP), kinematic constraints must be imposed.

For the sake of conciseness, the details of the dynamic equations and kinematic constrains are described in detail here but they can be found in Preidikman et.al. (2006).

2.4 Fluid Loading Effect

The effect of the external fluid on the dynamics of the IMP is incorporated through equivalent mass and moments of inertia in its equations of motion, i.e. an inertia matrix due to fluid loading is "added" to the inertia matrix in eq.(17). This is accomplished by finding the pressure distribution over the surface of the cylinder due to a rigid body motion or rotation when the body is immersed in a fluid (Cremer et.al., 1988; Fahy F., 1985, Junger and Feit, 1986). Once the pressure distribution as a function of frequency is obtained, the mechanical impedance is then computed as a function of frequency. The impedance values are then used to determine the equivalent added mass and added moment of inertia. The equivalent fluid mechanical-impedance terms will be determined from the closed form solution of the cylinder embedded in a baffle as shown in Figure 2. The IMP will then be allowed to independently move in the u_y and ϕ_y directions and the equivalent mechanical impedance terms computed. The same impedance values can be used in the *z*-direction, i.e. for u_z and ϕ_z. Since the fluid is assumed inviscid (no viscosity), it does not contribute to the mass in the *x*-direction and the polar moment of inertia about the *x*-axis. Once again the fluid is assumed to be at rest for this analysis. The IMP is modeled as a cylinder of radius *a* and length *L* as shown in Figure 2. To compute the pressure distribution, a baffled cylinder model is used. The infinite baffles are used in order to have an infinite-length function for the displacement in the *x*-direction. This makes possible the use of the wavenumber transform.

For the sake of conciseness, the details of the computation of the fluid loading can be found in Preidikman et.al. (2006).

3 LINEARIZATION OF THE EQUATIONS OF MOTION

To solve the equations of motion, they are first linearized about the near equilibrium position. In general, the linearized equations of motion of a nonconservative system are of the form

$$\mathbf{M}\,\ddot{\mathbf{x}} + \mathbf{D}\,\dot{\mathbf{x}} + \mathbf{K}_C\,\mathbf{x} - P\,\mathbf{K}_G\,\mathbf{x} = \mathbf{0} \tag{21}$$

where $\mathbf{M}$, $\mathbf{D}$, $\mathbf{K}_C$, and $\mathbf{K}_G$ are the mass, damping, elastic, and geometric matrices of dimension $n \times n$, respectively, and P is the load parameter. The matrices $\mathbf{M}$, $\mathbf{D}$, and $\mathbf{K}_C$ are symmetric. For nonconservative systems $\mathbf{K}_G$ is not symmetric, i.e. $\mathbf{K}_G \neq \mathbf{K}_G^T$. Modal expansion is applied for the solution of the system in eq.(21). Using the undamped eigenvalues ω_{i0}, and eigenvectors $\boldsymbol{\xi}_{i0}$ ($i = 1, \ldots, n$), the modal equations become

$$\ddot{q}_i + d_i\,\dot{q}_i + \omega_{i0}^2\,q_i - P\sum_{j=1}^{n} b_{ij} q_j = 0, \quad i = 1, 2, \ldots, n. \tag{22}$$

where d_i is the damping coefficient for the *i*-th mode.

Seeking a solution of the form $\mathbf{q}(t) = \boldsymbol{\zeta} e^{\lambda t}$ and substituting into eq.(22) results in

$$\left(\lambda^2 \mathbf{I}_{n\times n} + \lambda \mathbf{d} + \boldsymbol{\omega}_0^2 - P\,\mathbf{b}\right)\boldsymbol{\zeta} = \mathbf{0} \tag{23}$$

where $\mathbf{b}$ is a full matrix and

$$\boldsymbol{\omega}_0^2 = diag\left\{\omega_{10}^2, \omega_{20}^2, \ldots, \omega_{n0}^2\right\}, \qquad \mathbf{d} = diag\left\{d_1, d_2, \ldots, d_n\right\} \tag{24}$$

In order to have non-trivial solutions, the determinant of the coefficient matrix (a lambda-matrix) must be zero, i.e.

$$\det\left(\lambda^2\mathbf{I}_{n\times n}+\lambda\mathbf{d}+\boldsymbol{\omega}_0^2-P\mathbf{b}\right)=0 \tag{25}$$

which leads to a polynomial equation of degree $2n$ in λ. The roots of eq.(25) are in general complex numbers of the form $\lambda(P)=\alpha(P)\pm i\omega(P)$. Depending on the change of the eigenvalues $\lambda(P)$ as the load parameter P is increased, instability of the structure can occur. In our case, as it will be shown in the results section, when the load parameter $P=0$, the eigenvalues are purely imaginary. If two adjacent frequencies, say $\omega_r(P)$ and $\omega_s(P)$, come together when P increases, one has a double root $\omega_r(P_{crit})=\omega_s(P_{crit})=\omega_{crit}$ at $P=P_{crit}$. The response of the system, from these two critical modes, is of the form

$$q_{crit}(t)=(A+Bt)\sin(\omega_{crit}t)+(C+Dt)\cos(\omega_{crit}t) \tag{26}$$

which is oscillatory and with amplitude growing linearly with time. Since the instability is contributed by two modes, this is known as *coupled-mode flutter*. The coalescence of the eigenvalues is used to determine the stability of the system.

4 NUMERICAL RESULTS

The approach developed in the previous sections was implemented in a computer code. As an illustrative example of application of the numerical/computational tool developed in this effort, a case without damping is considered. As shown in Figure 4, when the load parameter $P=0$ the eigenvalues are purely imaginary. Because of the symmetry of the IMP and the isolators, $\omega_1=\omega_2$ and $\omega_4=\omega_5$. In this particular case, the adjacent frequencies $\omega_1(P)=\omega_2(P)$ and $\omega_4(P)=\omega_5(P)$ come together when P reaches the critical value $P=57.366$. At that point one has double roots (actually quadruple roots in our case, due to the symmetry mentioned) $\omega_1(P_{crit})=\omega_2(P_{crit})=\omega_4(P_{crit})=\omega_5(P_{crit})=\omega_{crit}=0.6451$ (see Figure 4). The response of the system from these critical modes is oscillatory and grows linearly with time as shown in Figures 5 and 6.

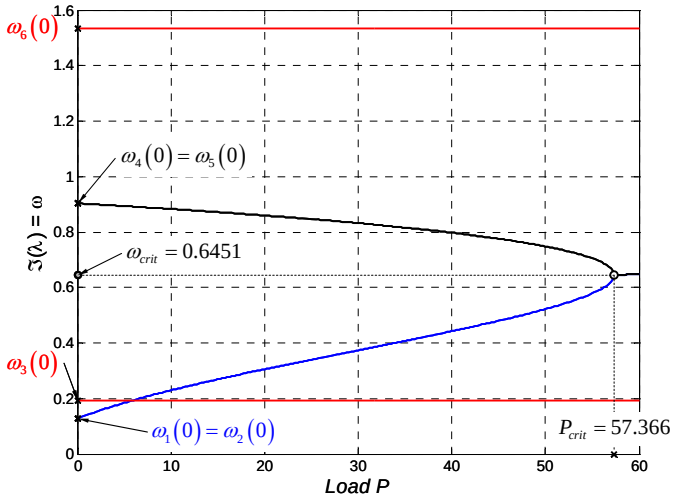

Figure 4: Coupled-mode flutter – Changes of the eigenvalues with the load parameter

The effect of damping can be easily included. It has been proved by Kelvin that damping has a stabilizing effect for conservative (non-gyroscopic) systems. However, it is important to mention that for nonconservative systems damping can have a destabilizing effect. Therefore, it is noted that for conservative systems it is safe in practice to neglect small damping in analysis and design. This is not the case for nonconservative systems; even a small damping may lead to a significant drop in the load that the structure is able to carry.

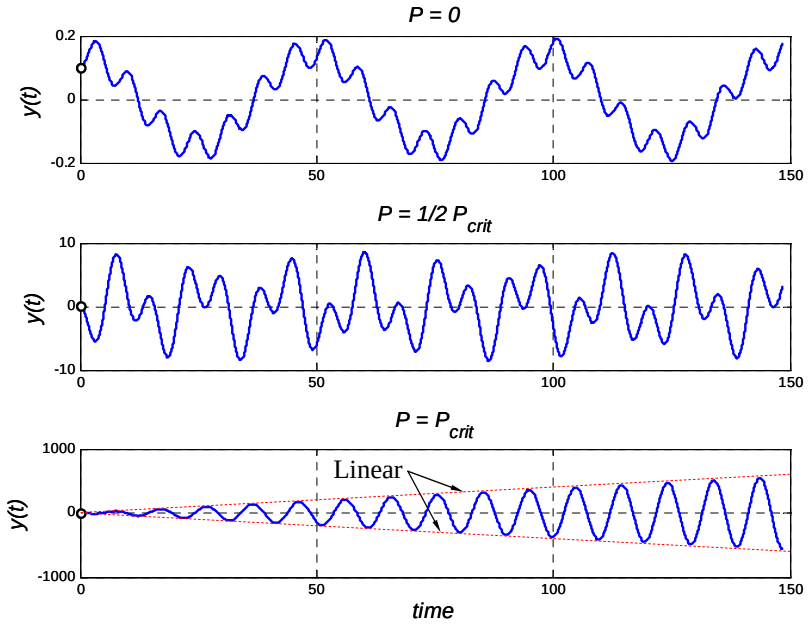

Figure 5: Coupled-mode flutter – Subcritical and critical responses: $y(t)$

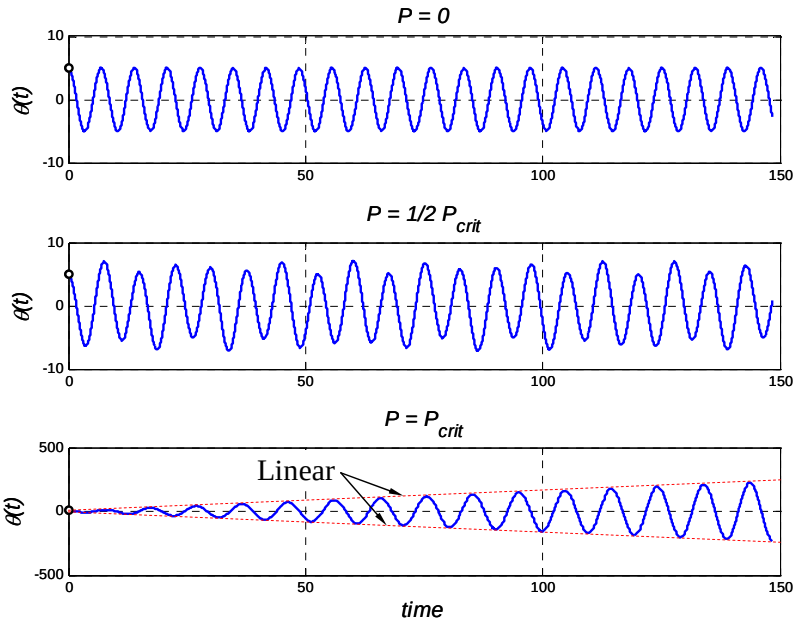

Figure 6: Coupled-mode flutter – Subcritical and critical responses: $\theta(t)$

5 CONCLUSIONS

The theoretical formulation for the dynamic stability analysis of soft mounted IMP systems was developed. The closed form approach developed here accounts for most of the physical aspects of the problem. The IMP is considered as a rigid body, the soft mounts are modeled as elastic beams, the external fluid-loading effects are incorporated as inertial terms, and the thrust as a follower force is modeled. The formulation was numerically implemented in a computer code and an example was presented. The stability of the system can be determined by inspections of the time history responses and/or an eigenvalue analysis, e.g. coalescence of natural frequencies.

The formulation can be improved in several aspects. However, there are two main improvements possible. Firstly, the formulation developed here allows identifying onset of instability (due to the linearization of the problem). However, it does not allow establishing if the instability will evolve into a limit cycle. This post-critical response requires the solution of the non-linear model. Secondly, the dynamic effect of the spinning propeller will have a stabilization effect (the degree of which is not known) that it is not accounted for in this formulation. This effect can be incorporated by including the gyroscopic stiffness matrix for the propeller.

REFERENCES

Abu Sharkh S.M., Lai S.H. and Turnock S.R., Structurally integrated brushless PM motor for miniature propeller thrusters, *IEE Proc.-Electr. Power Appl*., Vol. 151, No. 5, September 2004.

Baruh H., *Analytical Dynamics*, McGraw Hill. Boston, 1999.

Brown, D.W., Repp, J.R., and Taylor, O.S., Submersible outboard electric motor/propulsor, *Nav. Eng. J*., , 101, pp. 44–52, 1989.

Cremer L., Heckl M., and Ungar E. E., *Structural-Borne Sound*, 2nd Edition, Springer-Verlag, Berlin. 1988.

Fahy F., *Sound and Structural Vibration*, Academic Press, London. 1985.

Junger M. C. and Feit D., *Sound, Structures and Their Interaction*, 2nd Edition, MIT Press, Boston. 1986.

Meirovitch L., *Methods of analytical dynamics*, McGraw-Hill. New York, 1970a.

Meirovitch L., *Computational methods in structural dynamics*, Sijthoff & Noordhoff International Publishers. The Netherlands. 1980b.

Milne-Thomson L. M., *Theoretical Aerodynamics*, Dover Publications Inc., New York, 1958.

Preidikman S., Ravetta P., and Burdisso R. *Dynamic Stability Analysis of Isolated Integrated Motor Propulsor*, AVEC Final Report, October, 2006.

Rocard Y. and Meyer M. L., *Dynamic Instability: Automobiles, Aircraft, Suspension Bridges*, Ungar Publishing, 1958.

Wei-Chau Xie, *Dynamic Stability of Structures*, Cambridge University Press. UK. 2006.